

DETERMINING THE INTRINSIC KINETICS OF FISCHER–TROPSCH SYNTHESIS OVER COBALT CATALYST SUPPORTED ON FUNCTIONALIZED CARBON NANOTUBES

Behnam Hatami^{1,3}, Alireza Asghari¹, Ahmad Tavasoli²

¹ *Chemistry Department, Faculty of Science, Semnan University, Semnan, Iran*

² *School of Chemistry, College of Science, University of Tehran, Tehran, Iran*

³ *Gas Research Division, Research Institute of Petroleum Industry, Tehran, Iran*

Received July 27, 2016; Accepted November 7, 2016

Abstract

Intrinsic kinetics of Fischer–Tropsch (FT) reaction over cobalt catalyst supported on functionalized carbon nanotubes composes conversion of synthesis gas into liquid hydrocarbons is studied in a fixed bed microreactor. The reactor tests were done in 200–240°C, 15–30 bars, H₂/CO ratios of 1–2.5 and feed flow rates of 0.5–1.5 nL/g cat.hr. For presenting proper kinetics model for reactants' consumption, four different mechanisms were considered as probable mechanisms of Fischer–Tropsch reaction. Rate equations were obtained based on Langmuir - Hinshelwood model. For each proposed kinetic model, equilibrium constants and rate constants were extracted, and statistical analysis was used for comparing the mentioned values considering a rate limiting step. Finally, the rate equation for $r = \frac{k_4 K_1 K_2 K_3 P_{CO} P_{H_2}}{(1 + K_1 P_{CO})^2}$ which is extracted based on hydrogen assisted CO dissociation mechanism was considered as the most suitable equation for estimating the consumption rate of reactants. The activation energy was determined via Arrhenius equation for Co /CNTs catalyzed FTS as 184.28 (kJ/mol).

Keywords: Fischer–Tropsch, Cobalt; Carbon nanotubes; Functionalization; Kinetic model.

1. Introduction

Fischer–Tropsch synthesis (FTS) is a catalytic process for producing hydrocarbons and liquid fuels from synthesis gas (a mixture of H₂ and CO). Metals used as a catalyst in this process include iron (Fe), cobalt (Co) and ruthenium (Ru). Due to the high cost of Ru and its limited sources, Ru is less considered as the FTS catalyst. Although Co is more expensive than Fe, it is used more than Fe due to its higher activity, higher resistance and lower activity in water-gas shift reaction [1–6]. The reaction of Co with supports such as alumina and silica creates non-reducible compounds such as aluminates and silicates. Carbon-based materials such as carbon nanotubes and carbon nanofibers were used as cobalt FTS catalyst support to avoid the formation of these compounds

Several studies were performed on the kinetics of cobalt catalyzed Fischer–Tropsch synthesis. Bhatelia *et al.* studied the FTS intrinsic kinetic of 25%Co0.27%Ru/ γ -Al₂O₃ catalyst. They presented a kinetic model based on the mechanism of hydrogen assisted CO dissociation [7]. Also, Co-Mn/TiO₂ catalyzed FTS kinetics was studied by Azadi *et al.* in a fixed bed reactor. Several mechanisms were provided, and the results of two kinetic models were considered as acceptable models based on the mentioned mechanisms [8]. In addition, the FTS mechanism over cobalt catalysts studied by other researchers introduces the hydrogen assistant CO dissociation as the only available mechanism [9].

In our previous studies, we used functionalized carbon nanotubes (CNTs) as cobalt FTS catalyst support. This catalyst showed proper activity, selectivity, and stability. The mentioned catalyst was tested in pilot scale for a long time at industrial conditions, and the results were

very suitable. This work aims to provide intrinsic kinetic data and determine the rate equation for FTS over Co/CNTs catalyst in the absence of heat and mass transfer limitations.

2. Experimental

2.1. Support preparation

2.1.1. Preparation and purification of CNTs

CNTs were synthesized through methane decomposition at 900°C over cobalt- molybdenum nanoparticles supported on nanoporous magnesium oxide (Co-Mo/MgO) by chemical vapor deposition (CVD) method [11]. The reaction of methane decomposition was conducted at atmospheric pressure with a holding time of 30 min. The raw CNTs often contain impurities, such as amorphous carbon, catalyst metals, and fullerene and graphite particles [12-13]. Thus these impurities in CNTs are one of the factors preventing access to its significant features and need to be eliminated before using as a catalyst support. The purification procedure was done as follows: The pristine CNTs sample was added to an 18% HCl solution and mixed for about 16 hr at ambient temperature. The resulting mixture was filtered and washed several times with distilled water until the pH of the filtrate was neutral. In order to achieve to further-purification, the prepared materials dissolved in 6 M nitric acid for 3 hr at 70°C. After that, the washing step was repeated as mentioned above for the HNO₃ treatment process. The resulting cake was dried at 120°C for 8 hr, and in order to eliminate the amorphous carbons, the temperature was increased to 400°C for 30 min [11,15]. The purity of the CNTs was about 95%, with their diameters and lengths ranging between 10-20 nm and 5–15 μm respectively.

2.1.2. Functionalization of CNTs

It is known that CNTs have a hydrophobic surface, which is prone to aggregation and precipitation in water in the absence of a dispersant/surfactant. Up to now, many efforts have been made to prepare water-dispersible CNTs and numerous methods for chemical functionalization of CNTs. In this research, 1g of pure CNTs were added to 150 ml H₂O₂ (30%) and sonicated with the probe sonicator for 15 min. Then, the mixture was put in a vertically held Pyrex reactor (length and diameter of 300 and 160 mm respectively) equipped with a gas sparger. A stream of gaseous ozone was continuously passed through the sample at a rate of 314 ml/min for 4 hr. The unreacted ozone gas from the reactor was scrubbed into a sodium iodide solution (5%) before venting to the atmosphere in a fume hood. The resulting mixture was then filtered through a 0.2 mm polycarbonate membrane and washed with methanol to remove the remaining H₂O₂. The product was dried in an oven at 120°C for 5 hr [15].

2.2. Catalyst preparation

The above produced functionalized CNTs were used as support for preparation of the catalyst. The concentration of cobalt was adjusted at 15wt.%. The catalyst was prepared by microemulsion technique with an aqueous solution of cobalt nitrate (Co(NO₃)₂.6H₂O %99, Merck). Nanoparticles were synthesized in a reverse microemulsion using a nonionic surfactant Triton X-100 (Chem-Lab), n-hexane (C₆H₁₄, Chem-Lab) as the oil phase and 1-Butanol (C₄H₉OH, Merck) as the co-surfactant. The water-to-surfactant molar ratio (W/S) was fixed at 0.5. After vigorous stirring, a microemulsion was obtained (15 min). Hydrazine was added in excess (Hydrazine/Co = 10) to improve nanoparticle formation in the core of the micelles by reducing the metal oxides. Then, the appropriate weight of support was added under stirring. During the 3 h of stirring, tetrahydrofuran (THF), an emulsion destabilizing agent, was added drop wise (1 ml/min). A quick addition could lead to fast particle agglomeration and uncontrolled particle deposition on the support. The mixture was left to mature and settle slowly overnight and then decanted. The solid sample was recovered by vacuum filtration using ashless filtration paper (Whatman1) and washed several times with distilled water and ethanol. In order to remove the remaining traces of surfactant and ammonia, the catalyst was dried at 120°C for 2 h and calcined under argon (Ar) flow at 450°C for 3 h and slowly exposed to an oxygen

atmosphere during the cooling step. The catalyst composition, nomenclature, and properties are listed in Table 1.

Table 1. Chemical composition, textural properties, and cluster sizes of the CNTs and calcined catalyst

Sample	Targeted cobalt value (wt. %)	Measured cobalt value (wt. %)	BET surface area (m ² /g)	Total pore volume (mL/g)	Average pore diameter (Å)	XRD d _{Co₃O₄} (nm)
Functionalized CNTs	-	-	271	0.67	104	-
Co/CNTs	15	14.93	195	0.54	112	13.1

2.3. Characterization

The FTIR absorption technique for confirming the formation of functional groups was conducted on a Bruker ISS-88. A smooth transparent pellet of 2.5% of CNTs mixed with 97.5% potassium bromide (KBr), was made and the infrared beam passed through this pellet. The measurement of metal loading of the calcined catalyst was performed using Varian VISTA-MPX inductively coupled plasma-optical emission spectrometry (ICP-OES) instrument.

Surface area, pore volume, and pores average diameter of the calcined catalyst was measured using an ASAP-2010 V2 Micrometrics system. The sample was degassed at 200 °C for 4h under 50 mTorr vacuum and its BET area, pore volume and pore diameter were determined. The morphology of the catalyst was studied by transmission electron microscopy (TEM) using a Philips CM20 (100 kV) transmission electron microscope equipped with a NARON energy-dispersive spectrometer with a germanium detector.

Sample specimen for TEM studies was prepared by ultrasonic dispersion of the catalyst in ethanol, and the suspension was dropped onto a carbon-coated copper grid. The phases and average particle size of the crystals present in the catalyst were analyzed by XRD using a Philips Analytical X-ray diffractometer (XPert MPD) with monochromatized Cu/K α radiation between 2 θ angles from 20° to 80°. The Debye–Scherer formula was applied to Co₃O₄ peaks at 2 θ = 36.8°, in order to calculate the average particle size.

The H₂-TPR profile of the catalyst was performed in order to study the reducibility of the metal species in the catalyst. The calcined catalyst sample (0.05 g) was first purged in a flow of Helium at 140 °C to remove traces of water and gasses exist in the catalyst and then cooled to 40 °C. Then, the TPR of the sample was performed using 5% H₂ in Ar stream at a flow rate of 40 ml/min at atmospheric pressure using Micrometrics TPD-TPR 2900 analyzer equipped with a thermal conductivity detector (TCD), heating at a linearly programmed rate of 10 °C/min up to 850 °C. The amount of chemisorbed hydrogen on the catalyst was measured using the Micromeritics TPD-TPR 290 system. 0.25 g of the sample was reduced under hydro-gen flow at 400 °C for 12 h and then cooled to 100 °C under hydrogen flow. Then the flow of hydrogen was switched to argon at the same temperature, which lasted about 30 min in order to remove the weakly adsorbed hydrogen. Afterward, the temperature programmed desorption (TPD) of the sample was obtained by increasing the temperature of the sample, with a ramp rate of 10 °C/min, to 400 °C under the argon flow. The TPD profile was used to determine the cobalt dispersion and its surface average crystallite size. After TPD of hydrogen, the sample was reoxidized at 400 °C by pulses of 10% oxygen in helium to determine the extent of reduction. It is assumed that CoO is oxidized to Co₃O₄. The calculations are summarized in Ref. [16].

2.4. Methodology- reactor tests

The reactor tests were done for determining the kinetic of Fischer–Tropsch process in a fixed bed micro-reactor. The reactor is made of stainless steel 361 in 45cm length and 3.8-inch diameter. In each experiment, 1 gr of catalysts diluted with silicon carbide (1/5 ratio) was loaded into the reactor. The reactor temperature is monitored via a PID-type temperature controller. A mixture of feed gasses including CO and H₂ were regulated by Brooks 5850/s-type mass

handlers and conducted to the reactor. The loaded catalyst was first reduced in hydrogen at 400°C and atmospheric pressure for 16 hours.

2.4.1. Tests for Eliminating Mass Transfer Resistances

In these tests, after reduction process, the reactor temperature is reduced to 180°C and feed gas flow including H₂ and CO in 2:1 ratio has entered the reactor, and reactor pressure is raised to 18 bars, and the temperature is raised to 220°C. Reaction tests were done for finding conditions in which there are no resistances of internal and external mass transfer. The tests were done by different catalysts in 0.179-0.775 mm average diameter, in 200-240°C and feed flow rates of 80-140 cm³/min. In each experiment, two chromatography devices (GC) were used for analyzing gaseous products as online GC and liquid products as offline GC.

2.4.2. Tests for Determining Intrinsic Kinetic

Table 2 shows required reactor tests for Fischer–Tropsch synthesis kinetic determining that were designed with Taguchi method. The experimental design is presented in table 2.

Table 2. Experiments design

Run	P(bar)	T(°C)	H ₂ /CO	GHSV (NL/g Cat.hr)
1	20	200	2	0.7
2	20	200	1.5	0.5
3	15	200	2	1
4	25	200	1.5	1.2
Catalyst changing				
5	30	210	1.5	0.5
6	30	210	2.5	1.2
7	15	210	2	0.7
8	15	210	1	0.7
Repeat	30	210	1.5	0.5
9	20	210	2	1
10	20	210	1	1.2
11	25	210	1.5	1.5
12	25	210	2.5	1
Catalyst changing				
13	15	220	1	0.5
14	15	220	2	1
15	20	220	2	0.5
16	20	220	1.5	1.5
Repeat	15	220	1	0.5
17	20	220	2.5	1.2
18	25	220	2.5	0.7
19	25	220	1	1.2
20	30	220	2	1
Catalyst changing				
21	25	230	1	0.7
22	25	230	2.5	1.2
23	25	230	2	1.5
24	15	230	1.5	0.5
Repeat	25	230	1	0.7
25	15	230	2.5	1
26	30	230	2	0.5
27	30	230	2.5	0.7
28	20	230	1	1.5
Catalyst changing				
29	15	240	1.5	1.2
30	20	240	2	0.7
31	20	240	2.5	0.5
32	30	240	1	0.7

In this table, the various parameters are brought in a set of reactor tests and values of these parameters in each test. Determining a kinetic model for Co/CNTsFTS catalyst were

done by 32 reactor tests and changing different operational conditions including temperature, pressure, feed flow, and proportion of gas in feed in fixed bed reactor. To ensure the catalyst stability after doing several reactor tests, after discharging liquid product of each reactor test upon changing temperature, pressure, intensity of input feed flow rate, the conditions related to further test was applied.

3. Results and discussion

3.1. CNTs characterization

Results of FTIR test are given in Figure 1. This figure shows the infrared spectrum of the purified carbon nanotubes and functionalized ones. The peak at 1601 cm^{-1} is observed due to the stretching mode of double-bonds (C=C) in the nanotube backbone. The coupling of functional groups to CNTs can be confirmed by the presence of a series of new vibrational bands at $3300\text{--}3600\text{ cm}^{-1}$ (OH). Although, the moisture in the sample and KBr pellets in the FTIR sample preparation, increases the intensity of these peaks. Peaks at 1771 cm^{-1} (C=O for carboxyl groups), 1262 cm^{-1} (C-O), $2850\text{--}2950\text{ cm}^{-1}$ (both C-H anti symmetric and symmetric stretch for CH_3 and CH_2), 597 cm^{-1} (C-H) are shown [15]. There is a peak at 597 cm^{-1} bands of C-H bending mode. The main reason for this peak is the defects which are formed when the CNTs is significantly functionalized. The infrared spectrum shows that the peaks of this sample are almost identical to pure CNTs except that the related C=O and carbonyl peak intensity are increased, which indicates that further functionalized surface is available.

CNTs have a hydrophobic surface, which is prone to aggregation and precipitation in water. The above functionalized CNTs can disperse easily in some polar solvents such as water, ethanol, and formaldehyde. There are certain numbers of carboxyl, hydroxyl, and amino groups on the outer walls that can form a hydrogen bond with polar solvents which improve CNTs dispersion in solution.

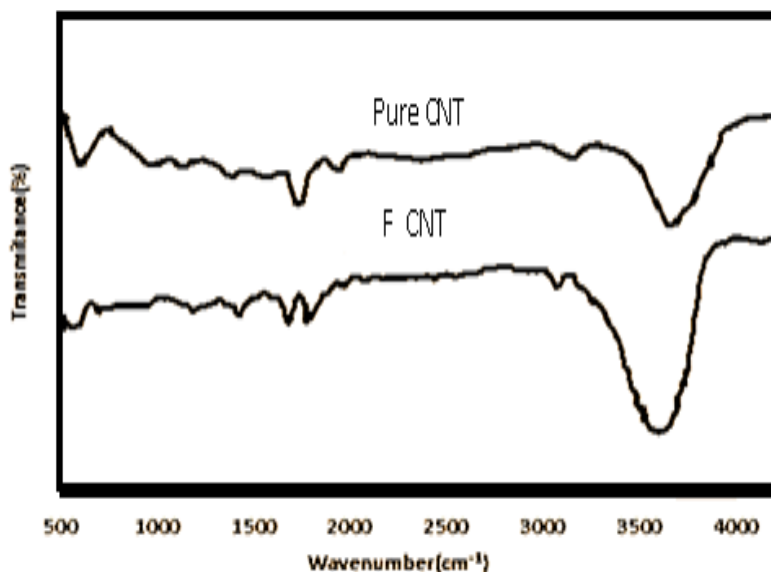


Figure 1. FTIR spectrum of common CNTs and functionalized CNTs support

3.2. Catalyst characterization

The elemental composition of the calcined catalyst measured by ICP is given in Table 1. This table shows that the metal content of the catalyst is fairly similar and close to the targeted metal content. Also, the results of BET and pore size distribution for the freshly calcined catalyst is shown in Table 1. According to these results, BET surface area for functionalized CNTs is significantly higher than that of the catalyst. As shown, loading of active metal, decreases the BET and pore volume, indicating some pore blockage. Also, for the catalysts with higher loadings

of active metals the average pore size shifted to higher values, suggesting that the smaller pores are partially blocked. The TEM image of the catalysis shown in Figure 2. TEM image demonstrates the spreading of the particles inside and outside of the CNTs channels. It seems that capillary forces led to confinement of cobalt particles inside the CNTs channels. This phenomenon can increase the BET surface area and dispersion of cobalt [17-20]. In this catalyst, the cobalt particles are dispersed mostly inside the tubes and the percentage of the particles lying on the outer surface of the functionalized CNTs is lower compared to the other catalysts. Figure 2 also depict the size distribution of the cobalt particles, which is determined using the population of the total cobalt particles of the catalyst based on data taken from different TEM images. This figure shows that the functionalized CNTs enable to perform a narrow cobalt nanoparticle size distribution because the surface functional groups act as anchoring sites for cobalt particles [21].

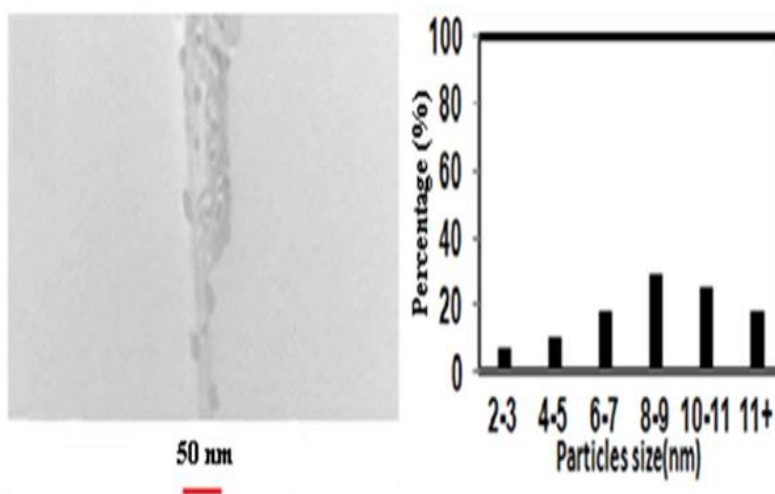


Figure 2. TEM images and particles size distributions for calcined catalyst

An XRD pattern of the calcined catalyst is shown in Figure 3. In the XRD pattern, the peaks at 2θ values of 25° and 43° correspond to the CNTs, while the other peaks in the XRD pattern of the catalyst are related to different crystal planes of Co_3O_4 [21]. The peak at 2θ value of 36.8° is the most intense one of Co_3O_4 in XRD of the catalyst. Minor peaks were also observed at 44° , and 52° for the catalyst which correlates with a cubic cobalt structure [17].

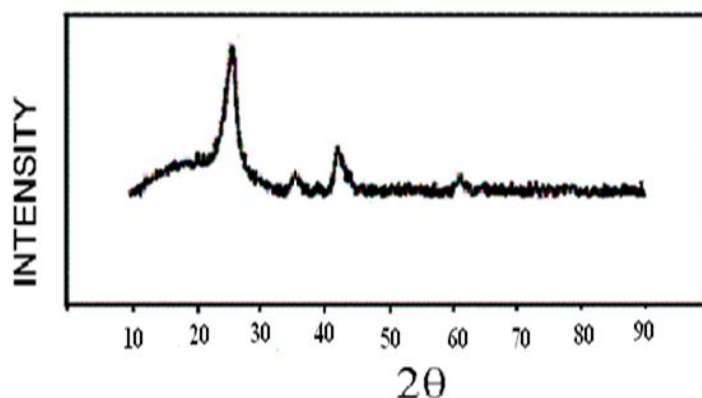


Figure 3. XRD patterns of calcined catalyst

Table 1 also shows the average Co_3O_4 particle size of the catalyst calculated from XRD pattern using Scherer formula at 2θ value of 36.8° [22]. According to this formula, the average Co_3O_4 cluster size is equal to 13.1 nm, corresponding to 9.8 nm when reduced to metal, respectively [22].

The results of hydrogen chemisorption test are given in Table 3. As shown, the average particles diameter determined by this method is in agreement with the results of XRD and TEM tests. Also, the percentage reduction and dispersion of the catalyst are suitable. Therefore, it can be concluded that functional groups play an important role in dispersion and degree of reducibility of cobalt particles on the functionalized CNTs. High dispersion and small cobalt cluster sizes will increase the number of sites available for CO conversion and hydrocarbon formation reactions.

Table 3. H₂ chemisorption results for the calcined catalyst

Sample	μ mole H ₂ desorbed/g cat.	μ mole O ₂ consumed/g cat.	Reduction (%)	Dispersion (%)	H ₂ -TPD d_{Co^0} (nm)
15Wt.% Co/CNTs Co/15	335	1505	64	22.35	9.6

The reducibility of the catalyst in H₂ atmosphere is determined by TPR experiments. The TPR spectra of the calcined catalyst and the specific reduction temperatures are presented in Figure 4. The low-temperature peak (301°C) is typically assigned to the reduction of Co₃O₄ to CoO, although a fraction of the peak likely comprises the reduction of the larger, bulk-like CoO species to Co⁰ [17]. The second broad peak (482°C) is assigned to the reduction of small CoO to Co⁰ species, which also includes the reduction of cobalt species that interact with the support. Deposited cobalt particles on the surface of functionalized CNTs will be easily reduced because of the confinement phenomenon and hydrogen spill-over the functional groups [22-23].

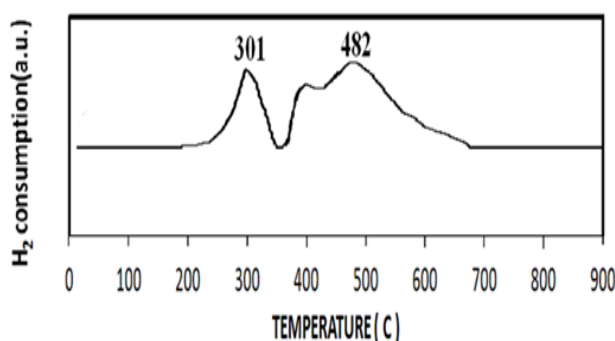


Figure 4. TPR patterns of calcined catalyst from 30 to 900°C

3.3. Results of Tests for Eliminating Mass Transfer Resistances

The reaction is performed due to the intrusion of reactants to the fluid layer encompassing the catalyst particles (external intrusion or film intrusion) and then into the catalyst pores (internal intrusion). The rate of a catalytic reaction without resistances of mass transfer is called intrinsic rate of the catalytic process. Establishing a fully messy flow in the reactor minimizes the external resistance to mass transfer or eliminates it.

Before intrinsic determination of reaction, the manner of influencing the flow intensity and size of catalysts on mass transfer were studied. Figure 5 shows a variation of carbon monoxide percentage conversion with catalyst particle sizes. As it is shown, reducing the size of catalyst particles will linearly increase the percent of carbon monoxide conversion. Reducing the size of catalysts from 0.775 mm to 0.255 mm increases the percent carbon monoxide conversion and further reduction of particles size to 0.175 mm, does not change the carbon monoxide conversion. According to these results, the size of catalyst particles has considerable effects on carbon monoxide conversion. For catalysts with less than 0.255 mm particles size, the internal resistance of mass transfer is negligible. Therefore, a catalyst with 0.255 μ m particles is chosen as a proper catalyst and was used for estimating kinetic equations.

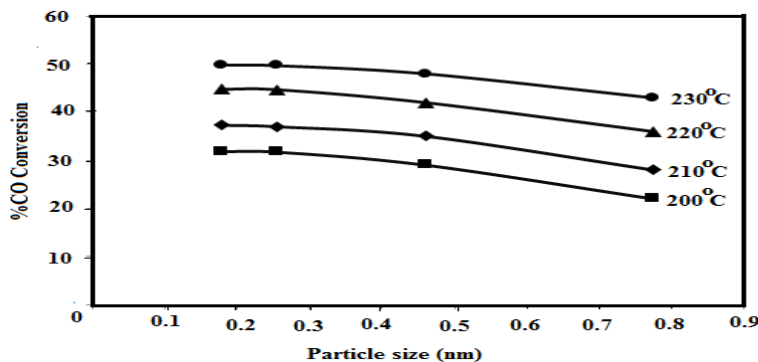


Figure 5. Variation of percentage carbon monoxide conversion with size of particles

To study the external mass transfer resistance, tests were performed at 220°C, 20bars and H₂/CO of 2 using 2gr of the catalyst with average particle size of 0.225 mm. Variation of percent CO conversion with changing the feed flow rate is shown in figure 6. When there is mass transfer resistance, increasing the feed flow rate reduces the thickness of the film for mass transfer and therefore increases the percent CO conversion. As show in this figure, increasing the flow rate from 80 to 140 mL/min reduces the conversion t from 52 to 41 which can be attributed to reducing the contact time of reactants with a catalyst in high feed flow rates. The values of mass transfer coefficients and film thickness (k_c and δ) were calculated for different flow rates [24]. The results are shown in table 4. These values show the negligible effect of feed flow rate on mass transfer coefficient in used test conditions.

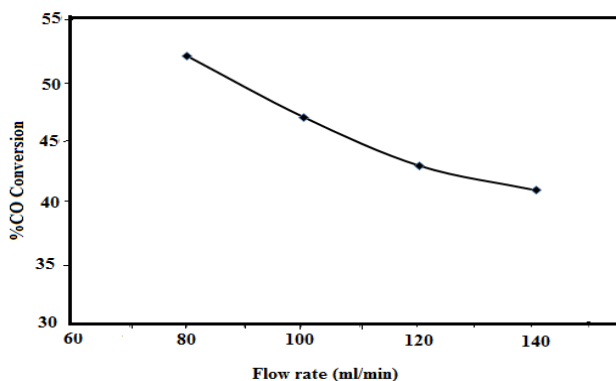


Figure 6. Variation of percent CO conversion with changing the feed flow rate

Table 4. Effect of Feed Flow Rate on External Mass Transfer

Flow rate(mL/min)	k_c (m/s)	δ (mm)
80	0.000994	0.054
100	0.00104	0.052
120	0.00108	0.050
140	0.00112	0.048

Also, in heterogenic catalytic reactions, C_{wp} is studied for determining the internal resistance of mass transfer. When $C_{wp} \leq 1$, there is no resistance to mass transfer and when $C_{wp} \geq 1$, the resistance of mass transfer is significant in the catalytic reaction. The parameter value can be computed via the following equation:

$$C_{wp} = \frac{-r_{A(obs)}\rho_c R^2}{D_e C_{AS}} \leq 1$$

in which $r_{A(obs)}$ is reaction rate in catalyst mass; R is the radius of the catalyst particle; ρ_c is catalyst density; C_{AS} is a concentration of A reactant in catalyst level and D_e is an effective intrusion.

The C_{wp} value was computed for the catalyst with 0.255 mm average particle size at 220°C which is obtained as 0.009. The obtained value is much less than 1, so it can be concluded that the mass transfer resistance for catalysts with 0.255 particle size is negligible.

3.4. Kinetic Studies, Estimating Parameters, and Statistical Tests

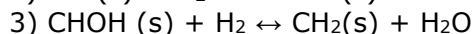
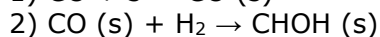
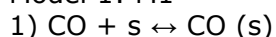
The experimental results of experiments are shown in table 5.

Table 5. Results of reactor tests

Run	-RCO (mol CO/gr cat.min)	Run	-RCO (mol CO/gr cat.min)
1	0.001724	Repeat	0.003224
2	0.001933	17	0.004803
3	0.002168	18	0.003965
4	0.002112	19	0.003685
5	0.003016	20	0.004032
6	0.003425	21	0.00259
7	0.006461	22	0.00275
8	0.008995	23	0.004965
Repeat	0.002995	24	0.006181
9	0.005664	Repeat	0.00251
10	0.004132	25	0.002223
11	0.002956	26	0.002632
12	0.003561	27	0.002556
13	0.003365	28	0.002478
14	0.005173	29	0.003705
15	0.004457	30	0.005108
16	0.004052	31	0.00658
		32	0.008451

For determining the rate equation, first the reaction mechanism is considered as primitive reactions comprising the total reaction, the mechanism of Fischer–Tropsch Process has always been considered and is challenging. Till now, different mechanisms were presented for justifying the formation of hydrocarbons via reaction of carbon monoxide and hydrogen in Fischer–Tropsch process. It is such that identifying the sequence of breaking available links in reactants and therefore creating new links and producing products are left as one of the unsolved problems in studying Fischer–Tropsch process. For kinetic determining, the Fischer–Tropsch process, mechanisms No. 1, 2, 3, 4 were considered as probable mechanisms (based on primitive reactions of reactants on catalytic active sites). For determining the rate equation based on each of the desired mechanisms, first one of the reaction steps is considered as slowest step and in fact as rate-determining step (RDS), and the rate equation related to this step is extracted, and the remaining steps are assumed as equilibrium and the equilibrium constants related to these steps are put in rate equation.

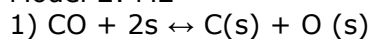
Model 1: M1



Equation 1:

$$\text{RDS 1: } r = \frac{k_2 K_{\text{CO}} P_{\text{CO}} P_{\text{H}_2}}{1 + K_{\text{CO}} P_{\text{CO}}}$$

Model 2: M2





Equation 2:

$$RDS\ 2: \quad r = \frac{k_3 K_{CO} P_{CO} (K_{H_2} P_{H_2})^2}{[1 + (K_{H_2} P_{H_2})^{1/2} + 2(K_{CO} P_{CO})^{1/2}]^6}$$

Model 3: M3

- 1) $CO + s \leftrightarrow CO(s)$
- 2) $H_2 + 2s \leftrightarrow 2H(s)$
- 3) $CO(s) + H(s) \rightarrow HCO(s) + s$
- 4) $HCO(s) + H(s) \leftrightarrow C(s) + H_2O(s)$
- 5) $C(s) + H(s) \leftrightarrow CH(s) + s$
- 6) $CH(s) + H(s) \leftrightarrow CH_2(s) + s$

Equation 3:

$$RDS\ 3: \quad r = \frac{k_3 K_{CO} P_{CO} K_{H_2}^{1/2} P_{H_2}^{1/2}}{(1 + K_{CO} P_{CO} + K_{H_2}^{1/2} P_{H_2}^{1/2})^2}$$

Model 4: M4

- 1) $CO + s \leftrightarrow CO(s)$
- 2) $H_2 + 2s \leftrightarrow 2H(s)$
- 3) $CO(s) + H(s) \leftrightarrow HCO(s) + s$
- 4) $HCO(s) + H(s) \rightarrow HCOH(s)$
- 5) $HCOH(s) + s \leftrightarrow CH(s) + OH(s)$
- 6) $OH(s) + H(s) \leftrightarrow H_2O + s$

Equation 4:

$$RDS\ 4: \quad r = \frac{k_4 K_1 K_2 K_3 P_{CO} P_{H_2}}{(1 + K_1 P_{CO})^2}$$

The rate parameters including rate constants and equation are computed via entering experimental rate and partial pressures of gasses in feed in the rate equations. The equation is solved via Polymath software. Table 6 shows the values of kinetic parameters related to different kinetic models. The equilibrium constant for absorbing carbon monoxide and rate constant related to model 1 in different temperatures show that increasing temperature reduces the equilibrium constant of CO absorption (K_{CO}) and increases the rate constant (k_2) and regarding the changes of equilibrium and rate constants, the kinetic model (1) is acceptable physically, so the accuracy of studied kinetic model is studied by statistical analyses. Comparing the values of kinetic parameters related to model 2 shows increasing of equilibrium constant of absorbing CO and H_2 upon increasing the temperature and such changes is not expected physically, so model 2 is considered as unacceptable. The values of K_{CO} and K_{H_2} related to model 3 increases with increasing temperature which shows the reduction of k_3 upon increasing the temperature. Also, the results show that k_3 is reduced with increasing the temperature. Such changes are impossible physically, so model 3 is unacceptable. The values of kinetic parameters in model 4, K_{CO} , K_{H_2} , K_{HCO} reduces upon increasing the temperature and k_4 increases with increasing temperature. So, kinetic model 4 is acceptable physically.

Table 6. Kinetic parameters

Temperature		200°C	210°C	220°C	230°C	240°C
M1	K_{CO}	0/31	0/239	0/113	0/028	0/00018
	k_2	0/00022	0/00126	0/00133	0/00337	0/525
M2	K_{CO}	2/86	2/89	1.3	2/5	2/33
	K_{H_2}	0/132	23/75	24/5	22/3	20/5
	k_3	0/951	212/7	216/5	245/2	280/1
M3	K_{CO}	1/51	0/79	1/79	2/97	3/2
	K_{H_2}	0/5	0/027	7/156	0/0066	0/23
	k_3	0/096	0/139	0/001029	43/1	50/2
M4	K_{CO}	4/4	4/2	4/1	3/8	2/4
	K_{H_2}	2/7	1/69	1/315	0/85	0/69
	K_{HCO}	0/031	0/024	0/00654	0/004	0/00032
	k_4	0/056	0/424	0/867	0/96	1/14

For measuring the accuracy of kinetic models 1 and 4, the statistical analyses including F-test, RMSE, *R*-squares were used, and the results of statistical tests are brought in table 7. According to the results, the *R*-squared related to M4 kinetic model is 0.611 which is more than the reported value for kinetic model 1 and this value is acceptable and statistically show that the experimental rates in-reactor tests and theoretical rate which are reported according to kinetic model 4 statistically are not remarkable different, The lower value of RMSE shows the possibility of using model in predicting the consumption rate of reactants. F-test statistical test was done for determining the difference of experimental and theoretical variances and statistically when $F(\text{model}) > F(\text{critical})$, it shows a significant difference in variance between two groups of data and such difference is unacceptable statistically. The results of F-test statistical test is brought in table 7. Regarding these results, model 1 does not provide a proper kinetic relationship for determining the rate of consumption of reactants in test conditions.

Table 7. Statistical analysis of kinetic models 1 and 4

	Model 1	Model 4
R squared	0.589	0.611
RMSE	0.00075	0.003831
F-test	4.24 > 2.4 (critical)	1.23 < 2.4 (critical)

Therefore, the statistical comparison of models 1 & 4 which is shown in table 7, the kinetic model 4 is the more proper kinetic model for predicting the consumption rate of reactants in Co/CNTs catalyzed Fischer–Tropsch process. The values of activation energy and absorption heat of reactants including CO and H₂ based on kinetic model 4 is obtained via Arrhenius relationship and are shown in table 8.

Table 8 Values of activation energy and absorption heat of CO and H₂

	K_{H_2} (kJ/mol)	K_{CO} (kJ/mol)	E(Activation energy) (kJ/mol)
Model 4	-23.41	-16.051	184.28

According to rate equation 4, the theoretical rate is computed at different temperatures including 200, 210, 220, 230, 240°C. Figures 7, 8, 9, 10 and 11 shows that kinetic model 4 predicts the theoretical rate values well.

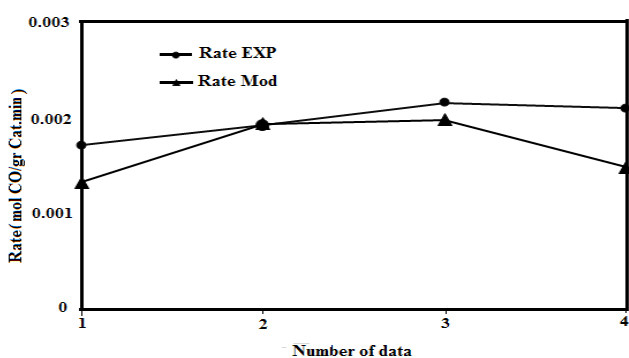


Figure 7. Comparing Theoretical & Experimental Rates of Reaction in 200°C

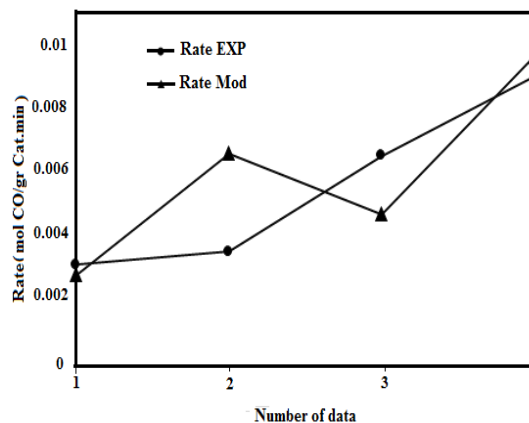


Figure 8. Comparing Theoretical & Experimental Rates of Reaction in 210°C

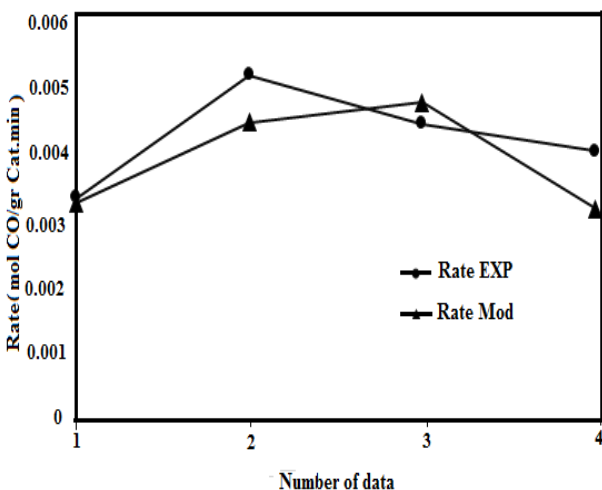


Figure 9. Comparing Theoretical & Experimental Rates of Reaction in 220°C

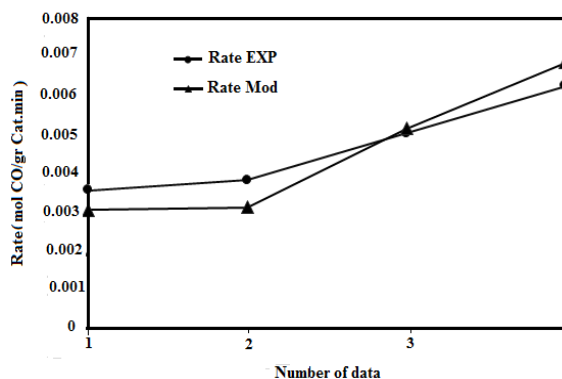


Figure 10. Comparing theoretical & Experimental Rates of reaction in 230°C

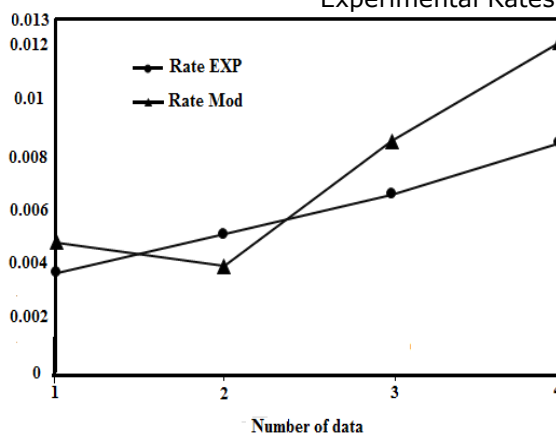


Figure 11. Comparing Theoretical & Experimental Rates of Reaction in 240°C

4. Conclusion

The rate equations related to reactants' consumption in Fischer-Tropsch process is studied according to Langmuir-Hinshwood model and RDS method. The rate equations were solved, and kinetic parameters values were obtained. The resulted models were compared physically by statistical tests and kinetic models 2 and 3 were not acceptable physically, and models 1 & 4 are considered as acceptable kinetic models physically. Determining the most proper model was done via statistical analysis. Model, 4 is presented as hydrogen assisted CO dissociation mechanisms on the catalyst, results in the most proper model and comparing the theoretical and experimental rates show the properness of mentioned model for predicting the consumption rate of reactants in the process.

References

- [1] Nel R, De Klerk A. *Fuel Chem.* 54 (2009) 118-119.
- [2] Schulz H. *App. Catal. A.* 186 (1999) 3-12.
- [3] Vosloo AC. *Fuel Proc Tech.* 71 (2001) 149-155.
- [4] Röper M and Loevenich H. *Catalysis in C1 Chemistry*, Reidel Publishing Company, Dordrecht 1983, pp. 41-88.
- [5] Khadakov A, Chu W. P. *Forgarland, Chem.Rev.* 107 (2007) 1692-1744.
- [6] Tavasoli A. *Catalyst composition and its distribution effects on the enhancement of activity, selectivity and suppression of deactivation rate of FTS cobalt catalysts*, Ph.D. Thesis, University of Tehran, 2005.

- [7] Bhatelia T, Ma. W, Davis. BH, Jacobs G and Bukur D. Chemical Engineering Transaction, 25(2011) 707-712.
- [8] Azadi P, Brownbridge G, Kemp I, Mosbach S, Dennis JS, Kraft M. ChemCatChem 2015, 7, 137 – 143
- [9] Tavasoli A, Abbaslou R, Trépanier M, Dalai AK. App.Catal. A. 345 (2008) 134-142.
- [10] Tavasoli A, Khodadadi A, Mortazavi Y, Sadaghiani K, Ahangari MG. Fuel Proc Tech87 (2006) 641–647.
- [11] Rashidi AM, Nouralishahi A, Khodadadi AA, Mortazavi Y, Karimi A, Kashefi K. Int. J. Hydrogen Energy, 35, 9489 (2010).
- [12] Li F, Cheng HM, Xing YT, Tan PH, Su G. Carbon, 38 (2000): 2041.
- [13] Andrews R, Jacques D, Qian D, Dickey EC. Carbon, 39 (2001) 1681-1687.
- [14] Zhang M, Yudasaka M, Iijima S. J. Phys. Chem. B, 108 (2004) 149.
- [15] Naeimi H, Mohajeri A, Moradi L, Rashidi AM. Appl. Surf. Sci., 256 (2009) 631.
- [16] Karimi A, Nasernejad B, Rashidi AM. Korean J Chem Eng 29 (2012) 1516–24.
- [17] Trepanier M, Tavasoli A, Dalai AK, Abatzoglou N. Appl. Catal. A, 353 (2009) 193.
- [18] Murugesan S, Myers K, Subramanian V. Appl. Catal. B: Environmental 103 (2011) 266–274.
- [19] Malek Abbaslou RM, Tavasoli A, Dalai AK, Appl. Catal. A: General 355 (2009) 33-41.
- [20] Karimi A, Nakhaei Pour A, Torabi F, Hatami B, Alaei M, Irani M. J. Nat. Gas Chem. 19 (2010) 503-508.
- [21] Bezemer GL, Van Laak A, Van Dillen AJ, De Jong KP. Stud. Surf. Sci. Catal. 147 (2004) 259-264.
- [22] Zhang Y, Liu Y, Yang G, Endo Y, Tsubaki N. Catal. Today, 142 (2009) 85.
- [23] Karimi A, Nasernejad B, Rashidi AM, Tavassoli A, Pourkhalil M. Fuel 117 (2014) 1045–1051.
- [24] Surisetty VR, Dalai AK, and Kozinski J. Energy Fuels 24(2010)4130–4137.

* Corresponding author Email: tavassolia@khayam.ut.ac.ir, Phone: (98)-21-61113643, Fax: (98)-21-66495291